Bioelectromagnetics 39:414–422 (2018)

Brief Communication

Numerical Evaluation of Human Exposure to WiMax Patch Antenna in Tablet or Laptop

Beatrice Siervo,[1] Maria Sole Morelli,[2] Luigi Landini,[1,3] and Valentina Hartwig [4]*

[1]*Department of Information Engineering, University of Pisa, Pisa, Italy*
[2]*Research Center "E. Piaggio," School of Engineering, University of Pisa, Pisa, Italy*
[3]*Fondazione CNR-Regione Toscana,"G. Monasterio," Pisa, Italy*
[4]*Institute of Clinical Physiology, CNR, Pisa, Italy*

The use of wireless communication devices, such as tablets or laptops, is increasing among children. Only a few studies assess specific energy absorption rate (SAR) due to exposure from wireless-enabled tablets and laptops, in particular with Worldwide Interoperability for Microwave Access (WiMax) technology. This paper reports the estimation of the interaction between an E-shaped patch antenna (3.5 GHz) and human models, by means of finite-difference time-domain (FDTD) method. Specifically, four different human models (young adult male, young adult female, pre-teenager female, male child) in different exposure conditions (antenna at different distances from the human model, in different positions, and orientations) were considered and whole-body, 10 and 1 g local SAR and magnetic field value (Bmax) were evaluated. From our results, in some worst-case scenarios involving male and female children's exposure, the maximum radiofrequency energy absorption (hot spots) is located in more sensitive organs such as eye, genitals, and breast. Bioelectromagnetics. 39:414–422, 2018. © 2018 Wiley Periodicals, Inc.

Keywords: FDTD; RF exposure; SAR; virtual population; WiMax; wireless communication device

INTRODUCTION

The use of wireless communication devices, such as tablets or laptops, is increasing among children. Worldwide Interoperability for Microwave Access (WiMax) is a communication system based on IEEE 802.16 [2004], belonging to fourth generation (4G) technology with well-known Long-term Evolution (LTE). Mobile WiMAX technology is an ideal means for a new generation of mobile Web applications since it allows mobile client machines to be connected to the Internet. The effects of electromagnetic (EM) radiation in the human body from communication devices have increasingly been taken into consideration in recent years. Specific absorption rate (SAR) is a standard dosimetric parameter [ICNIRP, 1998] for exposure to EM fields between 100 kHz and 10 GHz. SAR quantifies the absorbed energy providing whole-body heat stress and excessive localized tissue heating. Furthermore, SAR is proportional to the square of the internal electric field.

The International Commission on Non-Ionizing Radiation Protection (ICNIRP) has defined some reference levels from basic restrictions on induced whole-body-averaged SAR and peak 10 g spatial-averaged SAR [ICNIRP, 1998] to avoid potentially adverse health effects of EM fields in radiofrequency (RF) range (up to 300 GHz). The ICNIRP guidelines have been adopted by most countries. Generally, long-term EM field exposure is not considered in these guidelines, since consistent induction of cancer is not established. For this reason, ICNIRP guidelines consider only short-term, immediate health effects, such as elevated tissue temperatures resulting from absorption of energy during exposure to EM fields. These effects are produced above a certain threshold and this allows for setting some exposure limits for

Conflict of interest: None.

*Correspondence to: V. Hartwig, Institute of Clinical Physiology, CNR, Via G. Moruzzi 1, 56124 Pisa, Italy.
E-mail: valeh@ifc.cnr.it

Received for review 10 July 2017; Accepted 16 March 2018

DOI: 10.1002/bem.22128
Published online 30 April 2018 in Wiley Online Library (wileyonlinelibrary.com).

protectionist purposes. The ICNIRP exposure limits are based on available experimental evidence indicating that exposure of resting humans for approximately 30 min to EM fields produces a whole-body SAR of between 1 and 4 W/Kg, resulting in a body temperature increase of less than 1 °C. The limit for whole-body SAR is then reduced to 0.08 W/kg (1/50 of 1 degree heating) for the general public to account for sensitive subpopulations such as children and the elderly. Moreover, the limit for localized 10 g spatial-averaged SAR is set to 2 W/kg for the head and trunk and 4 W/kg for the limbs [ICNIRP, 1998].

More recent research has occurred in the field of EM exposure of children in addition to adults, without any firm conclusion. Morgan et al. [2014] concluded that children absorb a greater amount of microwave radiation than adults. Foster and Chou [2014] stated that age-related differences observed in worst case simulations are difficult to generalize to human populations under real-world exposure conditions. Several recent publications on cell phone dosimetry in children [Juutilainen et al., 2009; Christ et al., 2010a; Morris et al., 2015] reported higher SAR for children's brains compared to adults. Furthermore, Harris et al. [2011] reported results of numerical dosimetry for adult and children models exposed to signals of several wireless communication systems (UMTS, WiMax, and Bluetooth): they found that whole-body and localized SAR were lower than ICNIRP limits in all exposure conditions. On the other hand, whole-body average SAR values and local SAR for children were found to be higher than those of adults, under several exposure scenarios.

Actually, it is not only important to evaluate differences in SAR values between children and adults; rather, it is essential to foresee any "hot spots" that occur with RF exposure in the most sensitive parts of the body, such as eyes and genitals [Singh and Kapoor, 2014; Asghari et al., 2016].

The presence and position of these "hot spots" depend on the geometry and composition of the human body which are vary different with age and sex [Christ et al., 2010a; Markov and Grigoriev, 2015].

Currently, the most widely accepted computational method for SAR modeling is the finite-difference time-domain (FDTD) algorithm [Yee, 1966; Fernández-Rodríguez et al., 2015]: it offers great flexibility in modeling the inhomogeneous structures of anatomical tissues and organs with the possibility of estimating local SAR and detecting any "hot spots."

This paper reports the estimation, by means of FDTD method, of the interaction between an E-shaped patch antenna that works at 3.5 GHz (WiMax) and four different human models (young adult male, young adult female, pre-teenager female, male child) in different exposure conditions (antenna at different distances from the human model, in different positions and orientations), in terms of whole-body, 10 and 1 g local SAR, and magnetic field B.

METHODS

Antenna Model

In this study, E-shaped microstrip patch antenna was considered [Ramya et al., 2014]. Microstrip antennas have been used in the mobile phone and tablet market since they are low cost, easily fabricated, and have a low profile. The patch antenna had a global size of $25.7 \times 20.4\,mm^2$ and consisted of three layers: the ground plane, dielectric, and patch. The ground plane was made of perfect electric conductor (PEC). The dielectric was made of FR4 (NEMA, Rosslyn, VA) with thickness of 3.2 mm and a dielectric constant of $\varepsilon_r = 4.6$. The patch was made of copper with thickness of 0.7 mm. The antenna worked at a frequency of 3.5 GHz for WiMax. A sinusoidal voltage source (@ 3.5 Ghz, 1 V, 50 Ω) was placed on the patch surface as feed. The coefficient reflection S11 was—18.3 dB and VWSR = 1.28. The efficiency of the antenna was about 98.5% and its gain was 3.56 dBi. In Figure 1 (top), the patch antenna is shown and all dimensions are listed.

Human Models

Four available realistic human models (Duke, Ella, Billie, Thelonious) were used in our simulations. The models belonged to the Virtual Population (ViP) [Christ et al., 2010b] and were based on high resolution magnetic resonance (MR) images of healthy volunteers. Duke was a young adult male (age 34, height 1.77 m, mass 70.2 kg, BMI 22.4 kg/m^2, 146 tissues), Ella was a young adult female (age 26, height 1.63 m, mass 57.3 kg, BMI 21.5 kg/m^2, 76 tissues), Billie was a pre-teenager female (age 11, height 1.49 m, mass 34.0 kg, BMI 15.4 kg/m^2, 112 tissues), and Thelonious was a male child (age 6, height 1.15 m, mass 18.6 kg, BMI 14.1 kg/m^2, 76 tissues). The dielectric constant and conductivity for each specific tissue were calculated at 3.5 GHz [ITIS]. All the models were in standing position with arms by their side.

Numerical Simulations

All numerical simulations were performed with FDTD method using commercially available software XFdtd (Remcom, State College, PA). In our simula-

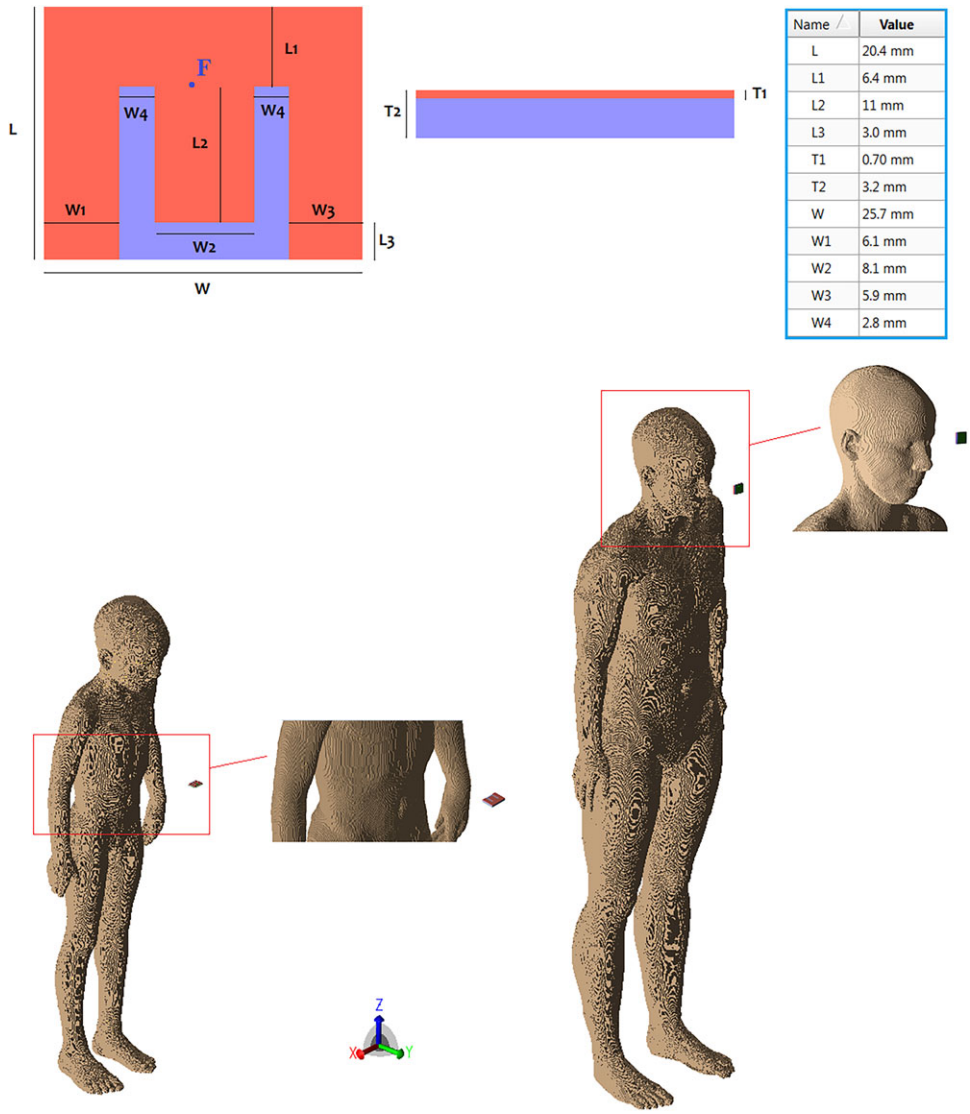

Fig. 1. **Top**: E-shaped microstrip patch antenna and its dimensions. F represents feed sinusoidal voltage source; **Bottom**: left side: Thelonious model with patch antenna at torso-level, far position, perpendicular orientation; **right side**: Ella model with patch antenna at nasion-level, near position, parallel orientation.

tions, an automatic non-uniform mesh was chosen with a maximum cell size of $2 \times 2 \times 2$ mm and a minimum of $1 \times 1 \times 1$ mm in the model volume. A time step of 3.84 ps was chosen, and the simulation was run for 100,000 steps with an automatic detection of convergence (@-30 dB). In order to truncate outward waves and therefore simulate infinite radiation boundary conditions of the computational domain, we used perfect matched layer (seven layers) [Duan et al., 2008] with 20 cells of free space that surrounded the voxel domain. All the simulations were performed using a computer Intel Core i5 at 2.67 GHz equipped with 4 GB of RAM, NVidia Geforce GTX 750 GPU card, and Windows 7 Home Premium x64 operating system. The simulations had an average duration of 22 min. We chose two positions for the patch antenna for the human model: the first at eye level, indicated with the term "nasion," and the latter at upper torso level, indicated with the term "torso." Furthermore, two different orientations were used: perpendicular orientation ($\perp$) and parallel orientation (//). For each position (nasion- and torso-level) and each orientation ($\perp$ and //), we chose two distances between the human model and antenna: closer position (near: 8 cm) and farther position (far: 16 cm). Perpendicular orientation of the patch antenna for the human model represents the exposure scenario in which the tablet or laptop is placed horizontally,

that is, placed on a table or desk. Otherwise, parallel orientation of the patch antenna for the human model represents the exposure scenario in which the tablet or laptop is placed vertically, that is, held in front of the head. Figure 1 (bottom) shows two examples of simulation scenario: Thelonious model with patch antenna at torso-level, far position, and perpendicular orientation; and Ella model with patch antenna at nasion-level, near position, and parallel orientation.

For each situation of exposure, local SAR in the entire model was estimated, specifically the peak local SAR, and 10 and 1 g averaged SAR. Afterwards, the magnetic field at the places where the maximum SAR was reported was estimated (Bmax).

RESULTS

Table 1 reports the maximum values of local whole-body SAR (SAR max), 10 and 1 g SAR values, and maximum values of magnetic field Bmax, for each human model and each exposure condition (perpendicular orientation: ⊥, parallel orientation: //). All the values reported are normalized for an input power of 1 W.

Table 2 shows local whole-body SAR maps in sagittal and axial planes (where SAR was maximum) for each human model and each exposure condition (different antenna position and distance from the human model). For all the cases described in Table 2, the patch antenna was oriented in a perpendicular way for the human model.

Table 3 shows local whole-body SAR maps in sagittal and axial planes (where SAR was maximum) for each human model and each exposure condition (different antenna position and distance from the human model) for parallel orientation of the patch antenna.

Figure 2 shows two of the simulated exposure conditions in which the maximum local SAR values are seen in more sensitive organs (eye and genitals): sagittal, axial, and coronal planes.

DISCUSSION AND CONCLUSION

In recent years, there has been a massive increase in the use of wireless communication systems. These wireless systems, such as LTE and WiMax, are able to increase the capacity and speed of mobile telephone networks. This strong growth has revealed the need to evaluate the human population's exposure to RF EM fields.

TABLE 1. Maximum Values of Local Whole-Body SAR, 10 and 1 g SAR Values, and Maximum Values of Magnetic Field Bmax for Each Human Model and Each Exposure Condition: Perpendicular and Parallel Orientation (@ Input Power = 1W).

		Nasion						Torso					
		Near			Far			Near			Far		
		SAR (W/kg)			SAR (W/kg)			SAR (W/kg)			SAR (W/kg)		
		Max	10 g	1 g	Max	10 g	1 g	Bmax (μT)	Max	10 g	1 g	Max	10 g	1 g	Bmax (μT)
⊥															
	Thelonious	4.11	0.32	1.15	0.31	1.26	0.10	0.36	0.17	1.38	0.15	0.52	0.41	0.91	0.11	0.35	0.48
	Billie	2.10	0.30	0.77	0.78	0.48	0.07	0.17	0.38	1.47	0.19	0.52	0.78	0.42	0.09	0.18	0.30
	Ella	1.51	0.26	0.56	0.54	0.44	0.07	0.16	0.16	1.22	0.12	0.27	0.46	0.51	0.07	0.15	0.28
	Duke	2.69	0.36	0.87	0.63	0.95	0.09	0.24	0.37	1.08	0.13	0.31	0.54	0.62	0.04	0.09	0.15
//																	
	Thelonious	11.35	1.09	3.86	1.69	3.15	0.32	1.09	0.54	4.59	0.53	1.20	0.79	1.17	0.16	0.37	0.36
	Billie	3.84	0.45	1.47	1.24	1.23	0.17	0.47	0.25	2.06	0.29	0.68	0.62	0.59	0.07	0.18	0.33
	Ella	3.90	0.45	1.36	0.79	1.32	0.14	0.42	0.43	2.04	0.22	0.48	0.63	1.15	0.10	0.23	0.25
	Duke	7.11	0.74	1.46	1.06	2.48	0.24	0.46	0.62	2.57	0.29	0.66	0.59	0.84	0.10	0.24	0.43

TABLE 2. Local Whole-Body SAR Maps in Sagittal and Axial Planes (Slices With Max Values) for Each Human Model and Each Exposure Condition: Perpendicular Orientation

	Nasion		Torso	
Perpendicular (⊥)	Near	Far	Near	Far
Thelonious	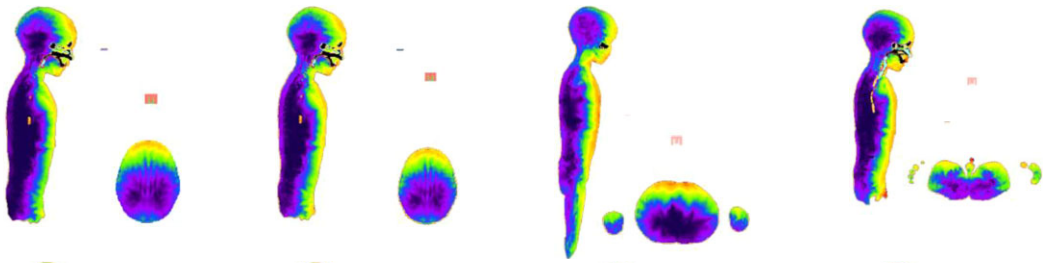			
Billie	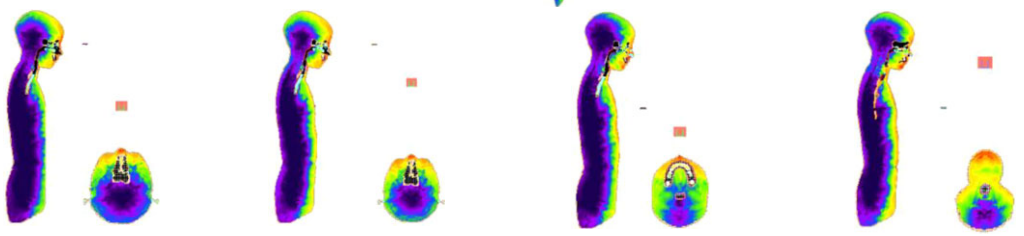			
Ella	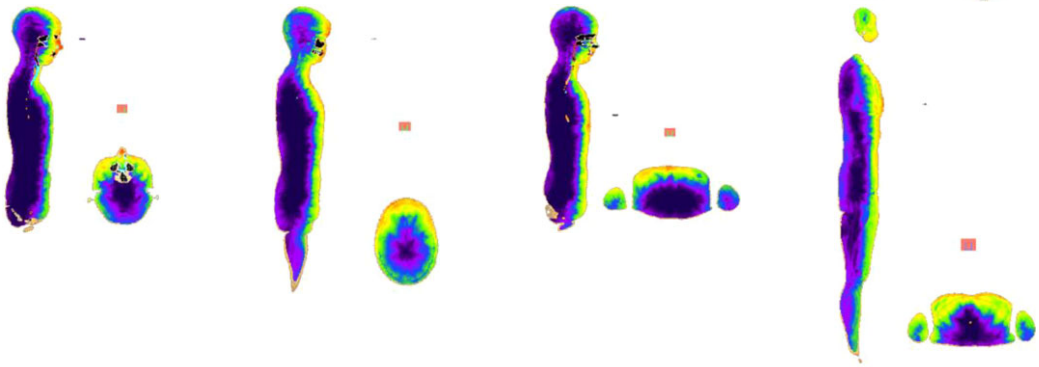			
Duke	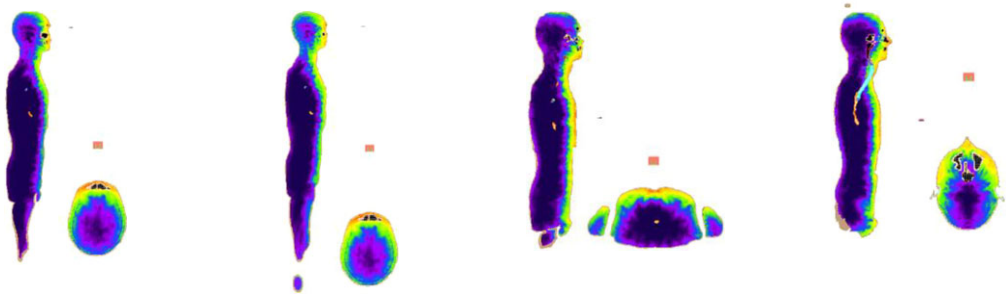			

Color scale is in arbitrary unit (from purple/minimum to red/maximum).

This paper describes numerical evaluation of SAR produced by a WiMax patch antenna in four realistic human models using FDTD numerical method. The FDTD method has been identified, in the IEEE Standards and Coordinating Committee 28 on Non-Ionizing Radiation Hazards [2008], as the preferred method for performing EM simulations for biological effects from wireless devices. FDTD predictions have been validated in several works both for simplistic geometric models [Gajšek et al., 2002; Stavroulakis, 2003] and more complex models such as human model [Homann et al., 2011; Wang et al., 2012], which have shown good qualitative and quantitative agreement. The considered antenna is typically employed in tablets or laptops and, generally, is positioned in the upper right side of the devices.

The SAR values presented in Table 1 have been normalized to an antenna output power of 1 W, while wireless antennas in laptops or tablets can generally

TABLE 3. Local Whole-Body SAR Maps in Sagittal and Axial Planes (Slices With Max Values) for Each Human Model and Each Exposure Condition: Parallel Orientation

	Nasion		Torso	
Parallel (//)	Near	Far	Near	Far
Thelonious	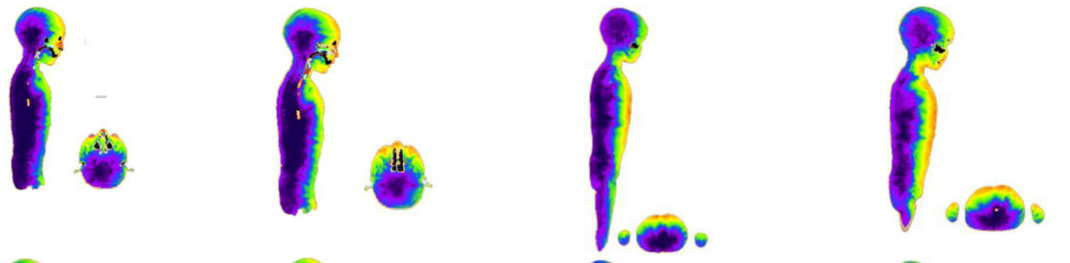			
Billie	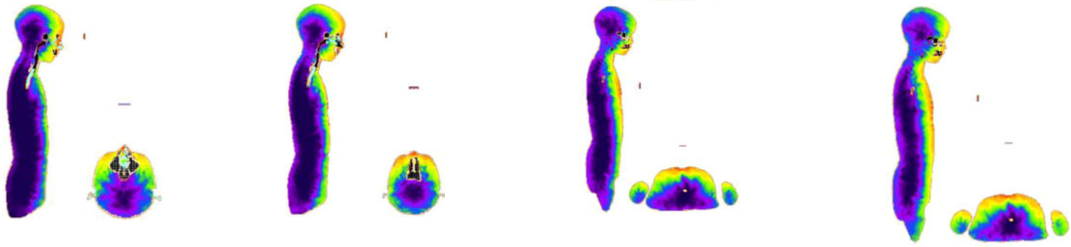			
Ella	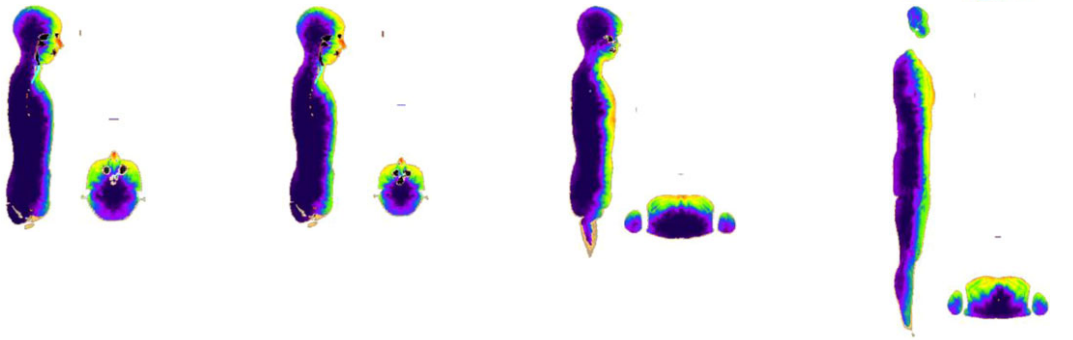			
Duke	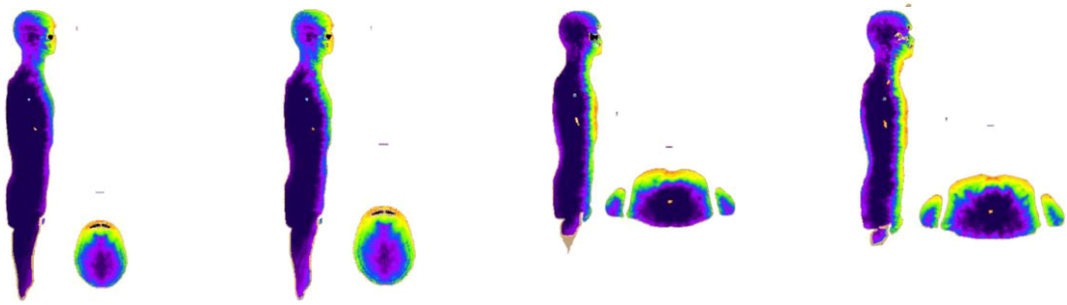			

Color scale is in arbitrary unit (from purple/minimum to red/maximum).

operate at a peak power of no more than 100 mW. Typically, a WiMAX antenna radiates a time-massed average power of 10 mW [Guterman et al., 2009; Findlay and Dimbylow, 2010].

After scaling, the calculated whole-body SAR exceeds the ICNIRP limits (0.08 W/kg) for only one exposure condition: male child exposed to EM field generated by the antenna placed at nasion-level in near position and parallel orientation (Table 2: SAR max = 0.11 W/kg @ 10 mW). This is a worst-case scenario at a very close distance (8 cm).

For all other cases, whole-body SAR and 10 g localized SAR do not exceed the safety limits.

Regarding the localization of the maximum values of SAR, Tables 2 and 3 show the "hot spots" for each exposure condition simulated in this study. It is possible that in some scenarios, maximum RF energy absorption is located in more sensitive organs, such as eyes and genitals. For example, maximum

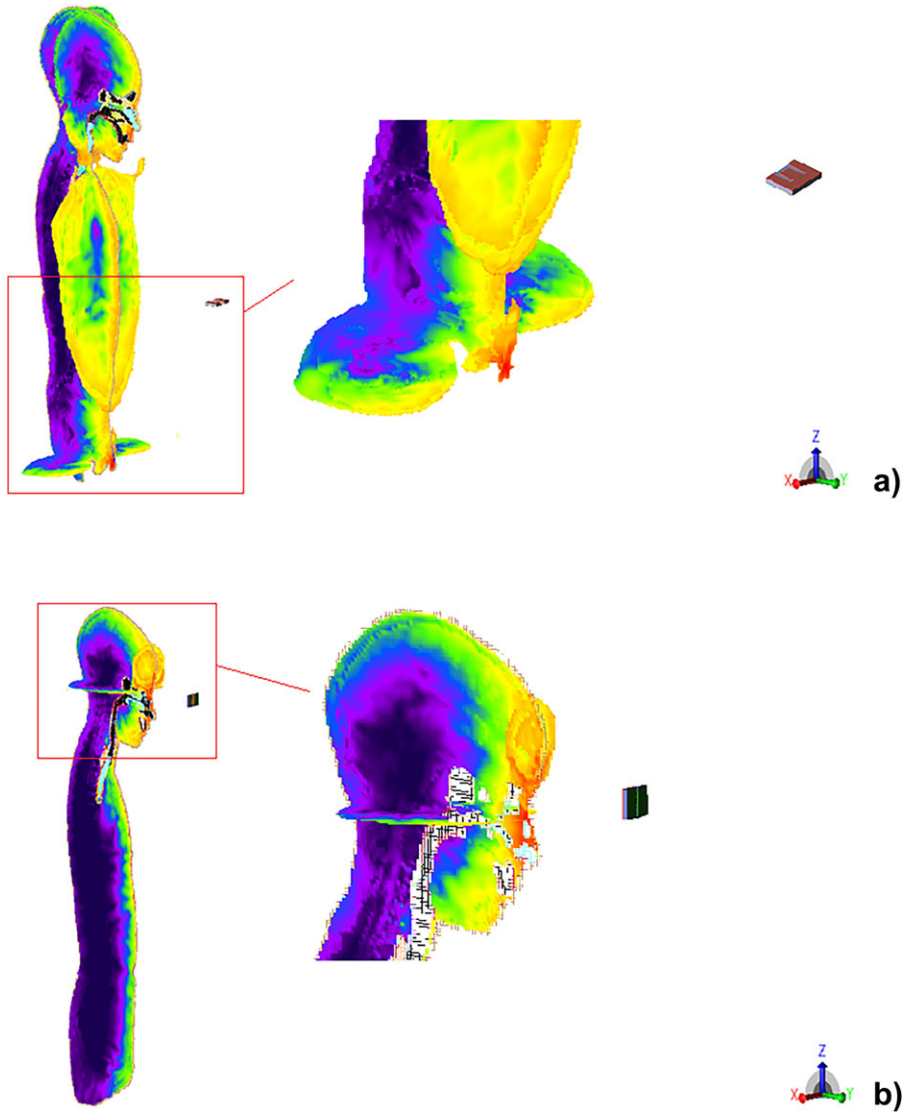

Fig. 2. Maximum local SAR in sagittal, axial, and coronal planes: (**a**) Thelonious, torso-level, far position, perpendicular orientation; (**b**) Billie, nasion-level, near position, parallel orientation. Color scale is in arbitrary unit (from purple/minimum to red/maximum).

value of local SAR is found in eye tissues for the following cases: Thelonious, nasion-level, near and far position, parallel orientation; Billie, nasion-level, near and far position, perpendicular, and parallel orientation. It has been established that one of the most sensitive organs for EM wave exposure is the human eye [Ng et al., 2012] and that the organ most sensitive to temperature is the eye lens [Markov, 2017].

The maximum SAR value is localized in genital organs when the male child model is exposed to the RF field generated by the E-shaped antenna, in perpendicular orientation at torso-level and at far position. This exposure condition represents a very likely scenario in daily life because it simulates the use of a laptop or tablet resting on a desk with the child standing in front of it. For this reason, this result needs particular attention since many studies have shown that EM fields can have destructive effects on male and female genital systems [Avendano et al., 2012; Shokri et al., 2015; Asghari et al., 2016].

Moreover, we found some exposure scenarios in which the maximum SAR value occurs in breast tissues when female models (Billie and Ella) were exposed to the EM fields at torso-level, at near or at far position, in parallel orientation. Since some cases of breast cancer due to prolonged contact between breast and EM RF field generators (cellular phones)

are present in the literature [Sage and Carpenter, 2009; West et al., 2013], this exposure condition should also be addressed in order to avoid any potential hazards, especially in teenagers, where growing breast tissue that occurs during puberty may be particularly vulnerable to EM exposure [West et al., 2013].

This study has one limitation since we used only the standing position for our human models without considering any different kind of posture such as sitting position or typing position. SAR values and locations could depend on the human model position [Guterman et al., 2009] and any additional elements such as laptop/tablet housing [Guterman et al., 2009].

In conclusion, the results of our study show the importance of simulating exposure taking into account the antenna-body mutual position for the exact localization of maximum SAR values ("hot spots"). Although the average SAR values do not exceed the recommended limits for all simulated exposure conditions except one, the maximum SAR values in some scenarios are located in more sensitive organs, which are the eyes, genitals, and breast. This is particularly important for children. Their entire organism is in a process of development and it is not possible to predict long-lasting problems that might occur as a result of exposure to EM fields at an early age. Nevertheless, recently Barnes and Greenenbaum [2016] presented possible theoretical mechanisms and experimental data concerning long-term exposures to RF magnetic fields, speculating that they can be responsible for changing in radical concentrations. Moreover, the values for the SAR reported here are expected to be in a range that could change the concentration of reactive oxygen species, and long-term exposures may be significant for some health effects [De Iuliis et al., 2009; Kang et al., 2014; Wang and Zhang, 2017].

Hence, until a more exhaustive monitoring of the potential risk of exposure from wireless-enabled devices is available, exposures of the young should be As Low As Reasonably Achievable (ALARA). To prevent any potential hazard and damage from the use of wireless devices, some simple rules, such as keeping the device as far away as possible from the eyes, genitals, and breast, should be established.

REFERENCES

Asghari A, Khaki AA, Rajabzadeh A, Khaki A. 2016. A review on Electromagnetic fields (EMFs) and the reproductive system. Electron Physician 8:2655–2662.

Avendano C, Mata A, Sarmiento C, Doncel G. 2012. Use of laptop computers connected to internet through Wi-Fi decreases human sperm motility and increases sperm DNA fragmentation. Fertil Steril 97:39–45.

Barnes F, Greenenbaum B. 2016. Some effects of weak magnetic fields on biological systems: RF fields can change radical concentrations and cancer cell growth rates. IEEE Power Electron Mag 3:60–68.

Christ A, Gosselin M-C, Christopoulou M, Kühn S, Kuster N. 2010a. Age-dependent tissue-specific exposure of cell phone users. Phys Med Biol 55:1767–1783.

Christ A, Kainz W, Hahn EG, Honegger K, Zefferer M, Neufeld E, Rascher W, Janka R, Bautz W, Chen J, Kiefer B, Schmitt P, Hollenbach H-P, Shen J, Oberle M, Szczerba D, Kam A, Guag JW, Kuster N. 2010b. The virtual family-development of surface-based anatomical models of two adults and two children for dosimetric simulations. Phys Med Biol 55: N23–N38.

De Iuliis GN, Newey RJ, King BV, Aitken RJ. 2009. Mobile phone radiation induces reactive oxygen species production and DNA damage in human spermatozoa in vitro. PLoS ONE 4:1–9.

Duan Y, Ibrahim TS, Peterson BS, Liu F, Kangarlu A. 2008. Assessment of a PML boundary condition for simulating an MRI radio frequency coil. Int J Antennas Propag 2008, Article ID 563196, 10.

Fernández-Rodríguez CE, De Salles AAA, Davis DL. 2015. Dosimetric simulations of brain absorption of mobile phone radiation-the relationship between psSAR and age. IEEE Access 3:2425–2430.

Findlay RP, Dimbylow PJ. 2010. SAR in a child voxel phantom from exposure to wireless computer networks (Wi-Fi). Phys Med Biol 55:N405–N411.

Foster KR, Chou CK. 2014. Are children more exposed to radio frequency energy from mobile phones than adults? IEEE Access 2:1497–1509.

Gajšek P, Walters TJ, Hurt WD, Ziriax JM, Nelson DA, Mason PA. 2002. Empirical validation of SAR values predicted by FDTD modeling. Bioelectromagnetics 23:37–48.

Guterman J, Moreira AA, Peixeiro C, Rahmat-Samii Y. 2009. Wrapped microstrip antennas for laptop computers. IEEE Antennas Propag Mag 51:12–39.

Harris L-R, Zhadobov M, Chahat N, Sauleau R. 2011. Electromagnetic dosimetry for adult and child models within a car: Multi-exposure scenarios. Int J Microw Wirel Technol 3:707–715.

Homann H, Bornert P, Eggers H, Nehrke K, Dossel O, Graesslin I. 2011. Toward individualized SAR models and in vivo validation. Magn Reson Med 66:1767–1776.

ICNIRP. 1998. ICNIRP guidelines for limiting exposure to time-varying electric, magnetic and electromagnetic fields. Health Phys 74:494–522.

IEEE. 2004. Air Interface for Fixed Broadband Wireless Access Systems, IEEE Std. 802.16.

IEEE. 2008. IEEE Std C95.3^{TM}-2002 (R2008): IEEE Recommended Practice for Measurements and Computations of Radio Frequency Electromagnetic Fields With Respect to Human Exposure to Such Fields, 100 kHz–300 GHz. Vol. 2002.

ITIS. Dielectric Properties. IT'IS Foundation. Available from: https://www.itis.ethz.ch/virtual-population/tissue-properties/database/dielectric-properties/. [Last accessed March 14, 2017].

Juutilainen J, Lagroye I, Miyakoshi J, van Rongen E, Saunders R, de Seze R, Tenforde T, Verschaeve L, Veyret B, Xu Z. 2009. Exposure to high frequency electromagnetic fields, biological effects and health consequences (100 kHz–

300 GHz). Rev Exp Stud RF Biol Eff (100 kHz–300 GHz) ICNIRP. Germany: Oberschleißheim. pp 90–303.

Kang KA, Lee HC, Lee J-J, Hong M-N, Park M-J, Lee Y-S, Choi H-D, Kim N, Ko Y-G, Lee J-S. 2014. Effects of combined radiofrequency radiation exposure on levels of reactive oxygen species in neuronal cells. J Radiat Res 55:265–276.

Markov M, Grigoriev Y. 2015. Protect children from EMF. Electromagn Biol Med 34:251–256.

Markov M. 2017. Dosimetry in Bioelectromagnetics. New York, NY: CRC Press. pp 1–428.

Morgan LL, Kesari S, Davis DL. 2014. Why children absorb more microwave radiation than adults: The consequences. J Microsc Ultrastruct 2:197–204.

Morris RD, Morgan LL, Davis D. 2015. Children absorb higher doses of radio frequency electromagnetic radiation from mobile phones than adults. IEEE Access 3:2379–2387.

Ng YKE, Tan JH, Acharya UR, Suri JS. 2012. Human Eye Imaging and Modeling. New York, NY: CRC Press. pp 1–430.

Ramya P, Gopalakrishnan S, Pradeep R. 2014. Modified E-shaped microstrip patch antenna for wimax application. Int J Adv Res Comput Commun Eng 3:7678–7680.

Sage C, Carpenter DO. 2009. Public health implications of wireless technologies. Pathophysiology 16:233–246.

Shokri S, Soltani A, Kazemi M, Sardari D. 2015. Effects of Wi-Fi (2.45 GHz) exposure on apoptosis, sperm parameters and testicular histomorphometry in rats: A time course study. Cell J 17:322–331.

Singh S, Kapoor N. 2014. Health implications of electromagnetic fields, mechanisms of action, and research needs. Adv Biol 2014:1–24.

Stavroulakis P. ed. 2003. Biological Effects of Electromagnetic Fields: Mechanisms, Modeling, Biological effects, Therapeutic Effects, International Standards, Exposure Criteria. Berlin, Heidelberg, Germany: Springer. pp 1–793.

Wang H, Zhang X. 2017. Magnetic fields and reactive oxygen species. Int J Mol Sci 18:E2175.

Wang J, Suzuki T, Fujiwara O, Harima K. 2012. Measurement and validation of GHz-band whole-body average SAR in a human volunteer using reverberation chamber. Phys Med Biol 57:7893–7903.

West JG, Kapoor NS, Liao S-Y, Chen JW, Bailey L, Nagourney RA. 2013. Multifocal breast cancer in young women with prolonged contact between their breasts and their cellular phones. Case Rep Med 2013:354682.

Yee KS. 1966. Numerical solution of initial boundary value problems involving Maxwell's equations in isotropic media. IEEE Trans Antennas Propag AP-14:302.